

The sample complexity of sparse multi-reference alignment and single-particle cryo-electron microscopy

Tamir Bendory and Dan Edidin

October 31, 2022

Abstract

Multi-reference alignment (MRA) is the problem of recovering a signal from its multiple noisy copies, each acted upon by a random group element. MRA is mainly motivated by single-particle cryo-electron microscopy (cryo-EM) that has recently joined X-ray crystallography as one of the two leading technologies to reconstruct biological molecular structures. Previous papers have shown that in the high noise regime, the sample complexity of MRA and cryo-EM is $n = \omega(\sigma^{2d})$, where n is the number of observations, σ^2 is the variance of the noise, and d is the lowest-order moment of the observations that uniquely determines the signal. In particular, it was shown that in many cases, $d = 3$ for generic signals, and thus the sample complexity is $n = \omega(\sigma^6)$.

In this paper, we analyze the second moment of the MRA and cryo-EM models. First, we show that in both models the second moment determines the signal up to a set of unitary matrices, whose dimension is governed by the decomposition of the space of signals into irreducible representations of the group. Second, we derive sparsity conditions under which a signal can be recovered from the second moment, implying sample complexity of $n = \omega(\sigma^4)$. Notably, we show that the sample complexity of cryo-EM is $n = \omega(\sigma^4)$ if at most one third of the coefficients representing the molecular structure are non-zero; this bound is near-optimal. The analysis is based on tools from representation theory and algebraic geometry. We also derive bounds on recovering a sparse signal from its power spectrum, which is the main computational problem of X-ray crystallography.

1 Introduction

This paper studies the multi-reference alignment (MRA) model of estimating a signal from its multiple noisy copies, each acted upon by a random group element. Let G be a compact group acting on a vector space V . Each MRA observation y is drawn from

$$y = g \cdot f + \varepsilon, \quad (1.1)$$

where $g \in G$, $\varepsilon \sim \mathcal{N}(0, \sigma^2 I)$ is a Gaussian noise independent of g , \cdot denotes the group action, and $f \in V$. We assume that the distribution over G is uniform (Haar). The goal is to estimate the signal $f \in V$ from n realizations

$$y_i = g_i \cdot f + \varepsilon_i \quad i = 1, \dots, n. \quad (1.2)$$

Evidently, it is impossible to distinguish between f and $\tilde{g} \cdot f$ for any $\tilde{g} \in G$, from the observations y_1, \dots, y_n , with no prior knowledge on f . Thus, we can only hope to recover the orbit of $f \in V$ under G .

A wide range of MRA models have been studied in recent years. The simplest and most studied model is when a signal in $V = \mathbb{R}^N$ is estimated from its multiple circularly shifted, noisy copies, namely $G = \mathbb{Z}_L$ [9, 18, 2, 11, 68]. Figure 1 illustrates observations drawn from this model. Additional MRA models include the dihedral group acting on \mathbb{R}^N [21], the group of two-dimensional rotations $\text{SO}(2)$ acting on band-limited images [10, 61, 49], the group of three-dimensional rotations $\text{SO}(3)$ acting on band-limited signals on the sphere [8, 60], as well as additional setups [69, 47, 22]. The results of this paper hold for any MRA model when a compact group G is acting on a finite-dimensional space V ; specific examples are provided in Section 2.4.

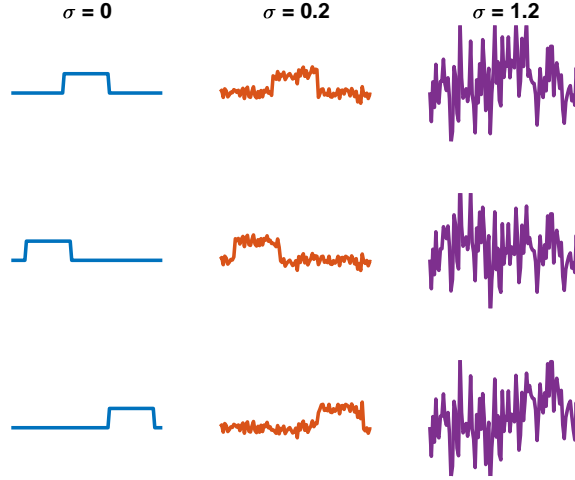


Figure 1: An example of the one-dimensional MRA setup where a signal in \mathbb{R}^N is acted upon by random elements of the group of circular shifts \mathbb{Z}_N . The left column shows three shifted copies of the signal, corresponding to noiseless measurements (i.e., $\sigma = 0$). In this case, all three observations are admissible solutions as the signal can be estimated only up to a group action. The middle and right columns present the same observations, with low noise level of $\sigma = 0.2$ and high noise level of $\sigma = 1.2$. This paper focuses on the extremely high noise level $\sigma \rightarrow \infty$ when the signal is swamped by noise. Figure credit: [14].

The MRA model is mainly motivated by single-particle cryo-electron microscopy (cryo-EM)—an increasingly popular technology that has joined X-ray crystallography as one of the two leading technologies to reconstruct molecular structures [43, 66]. Under some simplified assumptions, the cryo-EM generative model reads

$$y = T(g \cdot f) + \varepsilon, \quad g \in G, \quad (1.3)$$

where G is the group of three-dimensional rotations $\text{SO}(3)$, and T is a tomographic projection acting by

$$Tf(x_1, x_2) = \int_{\mathbb{R}} f(x_1, x_2, x_3) dx_3. \quad (1.4)$$

The celebrated Fourier Slice Theorem states that the 2-D Fourier transform of a tomographic projection is equal to a 2-D slice of the volume’s 3-D Fourier transform [64]. This motivates analyzing the cryo-EM model in Fourier space, which is indeed the common practice. Notably, the noise level in cryo-EM images is very high; Figure 2 shows several experimental cryo-EM images. We refer the reader to recent surveys on the mathematical and algorithmic aspects of cryo-EM [80, 14, 83].

While the linear random action of 3-D rotation followed by a tomographic projection does not constitute a group action, we will show that the results of this paper apply to the cryo-EM model as well. The emerging molecular reconstruction technology of X-ray free-electron lasers (XFEL) also obeys the model (1.3) with one important distinction: the phases in Fourier space are unavailable [85, 62].

MRA analysis in the high and low noise regimes. In the low noise regime, when the signal dominates the noise, the group elements $g_1, \dots, g_n \in G$ can be usually estimated accurately from the observations, see for example [79, 28, 33, 72, 59]. If we denote the estimated group elements by $\hat{g}_1, \dots, \hat{g}_n \in G$, then an estimator \hat{f} can be constructed by applying the inverse group elements and averaging:

$$\hat{f} = \frac{1}{n} \sum_{i=1}^n \hat{g}_i^{-1} y_i.$$

In cryo-EM, while the statistical model is more involved (1.3), the group elements can be estimated as well based on the common-lines geometrical property [82, 77], and thus recovering the molecular structure reduces to a linear inverse problem for which many effective techniques exist [64].

Motivated by cryo-EM, this work focuses on the high noise regime, when the signal is swamped by noise, and thus the group elements cannot be accurately estimated [16, 4, 71]. Consequently, one needs to develop methods to estimate the signal f directly, without estimating the group elements as an intermediate step. In particular, two main estimation methods dominate the MRA literature. The first is based on optimizing the marginalized likelihood function, using methods such as expectation-maximization [18, 61, 23, 21, 49, 55, 25]. While these techniques are highly successful, and are the state-of-the-art methods in cryo-EM [78, 74, 70], their properties are currently not well-understood [42, 53, 30, 41]. The second approach is based on the method of moments—a classical parameter estimation technique, tracing back to the seminal paper of Pearson [67]. In the method of moment, the idea is to find a signal which is consistent with the empirical moments (which are estimates of the population moments). The method of moments was applied to a wide range of MRA models [18, 8, 68, 2, 32, 29, 61, 69, 5, 47, 60, 23, 21, 25, 44, 1], as well as to construct ab initio models in cryo-EM [26, 27, 58, 75, 16, 56, 48] and XFEL [73, 35]. In this work, we focus on the method of moments due to its appealing statistical properties that are introduced next.

Sample complexity. In the high noise regime $\sigma \rightarrow \infty$, when the dimension of the signal is finite, it was shown that a necessary condition for recovery is $n = \omega(\sigma^{2d})$ (namely, $n/\sigma^{2d} \rightarrow \infty$ as $n, \sigma \rightarrow \infty$), where d is the lowest-order moment that determines the orbit of the signal

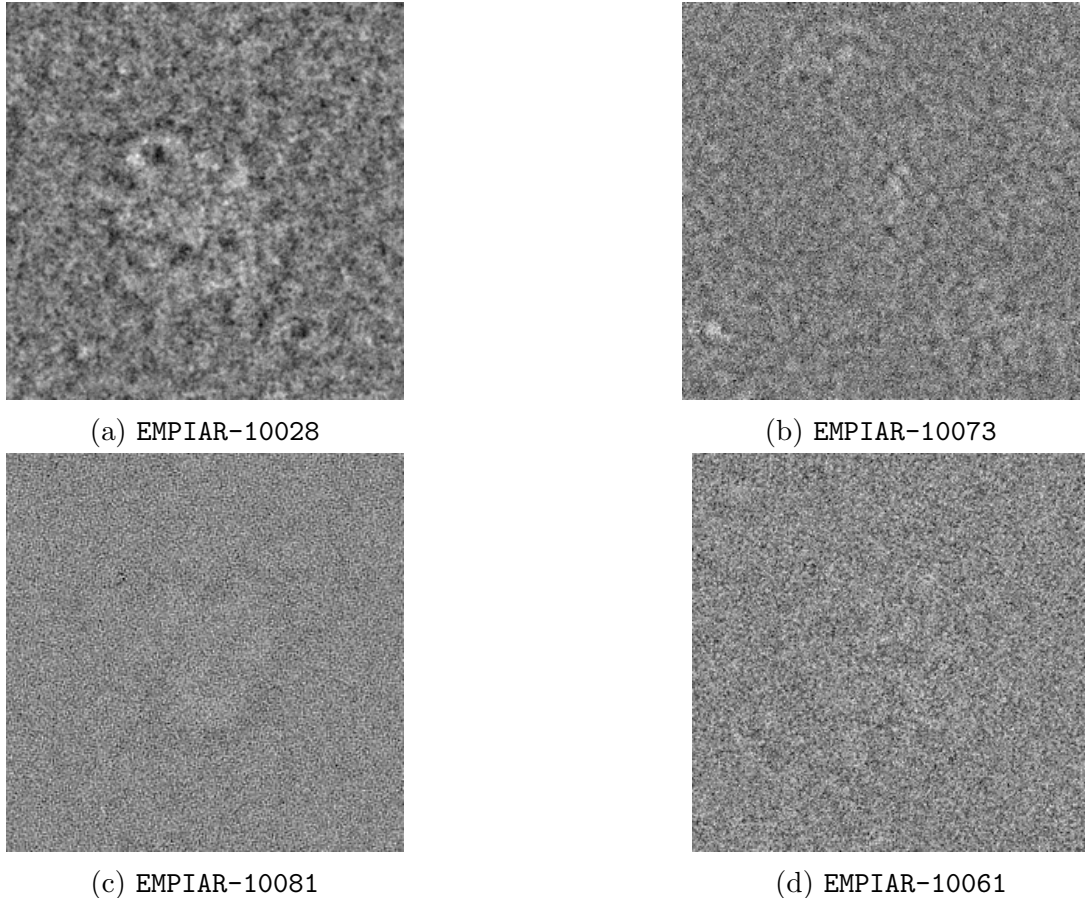


Figure 2: A collection of cryo-EM experimental images, taken from the the Electron Microscopy Public Image Archive (EMPIAR) <https://www.ebi.ac.uk/empir/>. The corresponding molecular structures are available at the Electron Microscopy Data Bank (EMDB) <https://www.ebi.ac.uk/emdb>. (a) EMPIAR-10028 (corresponding entry EMD-2660): *Plasmodium falciparum* 80S ribosome bound to the anti-protozoan drug emetine [89]; (b) EMPIAR-10073 (corresponding entry EMD-8012): yeast spliceosomal U4/U6.U5 tri-snRNP [65]; (c) EMPIAR-10081 (corresponding entry EMD-8511): human HCN1 hyperpolarization-activated cyclic nucleotide-gated ion channel [57]; (d) EMPIAR-10061 (corresponding entry EMD-2984): beta-galactosidase in complex with a cell-permeant inhibitor [12].

uniquely¹ [11, 3, 68]. In [8], it was shown that in many cases, if the distribution of the group elements is uniform (as we assume in this paper), $d = 3$ suffices to determine almost all signals, implying sample complexity of $n = \omega(\sigma^6)$; this is also true for cryo-EM. Moreover, in some cases, an efficient algorithm to recover the signal at the optimal estimation rate was devised. For example, if $V \in \mathbb{R}^N$ and $G = \mathbb{Z}_N$, a generic signal can be recovered efficiently from the third moment, called the bispectrum, using a variety of efficient algorithms [18, 68]; see also [60].

¹This is not necessarily true when the dimension of the signal grows with the noise level and the number of observations [71, 37].

We mention that when the distribution of the group elements is non-uniform, the MRA problem is usually easier, and signal recovery may be possible from the second moment [2, 21, 75]. In fact, uniform distribution can be thought of as the worst-case scenario of the MRA model (1.1) since, no matter what the original distribution over the group elements is, one can force a uniform distribution by generating a new set of observations:

$$z_i = \tilde{g}_i \cdot y_i = (\tilde{g}_i g_i) \cdot f + \tilde{g}_i \cdot \varepsilon_i, \quad (1.5)$$

where \tilde{g}_i is drawn from a uniform distribution (and thus the distribution of $\tilde{g}g$ is also uniform). This is not necessarily true for the cryo-EM model.

Main contributions: Signal recovery from the second moment. This work studies signal recovery from the second moment of the MRA observations:

$$\mathbb{E}yy^* = \int_G (g \cdot f)(g \cdot f)^* dg. \quad (1.6)$$

If we view $g \cdot f$ as a column vector, then $(g \cdot f)(g \cdot f)^*$ is a rank-one matrix, and thus the second moment is an integral over rank-one Hermitian matrices. Recall that the second moment can be estimated from samples

$$\mathbb{E}yy^* \approx \frac{1}{n} \sum_{i=1}^n y_i y_i^*. \quad (1.7)$$

When $n = \omega(\sigma^4)$, $\mathbb{E}yy^* = \frac{1}{n} \sum_{i=1}^n y_i y_i^*$ almost surely. Thus, identifying a class of signals that can be recovered from $\mathbb{E}yy^*$ will imply that the sample complexity of the problem, for this class of signals, is $n = \omega(\sigma^4)$ and not $n = \omega(\sigma^6)$ as for generic signals [8, 18, 68].

The first contribution of this paper, introduced in Section 2, is precisely characterizing the set of signals which are consistent with the second moment. Through the lense of representation theory, we show in Theorem 2.3 that the second moment determines the signal up to a set of unitary matrices, whose dimension is governed by the decomposition of the space of signals into irreducible representations of the group. While the unitary matrix ambiguities have been identified before in some special cases [52, 26], we show that the same pattern of ambiguities governs all MRA models. Section 2.4 provides specific examples.

To resolve these ambiguities, we suggest assuming the signal is sparse under some basis. This is a common assumption in many problems in signal processing and machine learning, such as regression [86, 45], compressed sensing [36, 31, 39], and various image processing applications [38]. Our second contribution, presented in Section 3 and summarized in Theorem 3.1, describes the sparsity level under which the orbit of a generic sparse signal can be recovered from the second moment. That is, the sparsity level that allows resolving the unknown unitary matrices. This implies that merely $n = \omega(\sigma^4)$ observations are required for accurate signal recovery. The sparsity level is bounded by a factor that depends on the dimensions of the irreducible representations and their multiplicities. The proof of Theorem 3.1 relies on tools from algebraic geometry and representation theory. Specific results are provided in Section 3.3.

Implications to cryo-EM. In Section 4, we show that the second moment of the cryo-EM model (1.3) is the same as of the MRA model (1.1), when G is the group of three-dimensional rotations $\text{SO}(3)$ and V is the space of band-limited functions on the ball. Namely, the tomographic projection operator (1.4) does not change the second moment of the observations. We introduce this model in detail in Section 4 and particularize the main result of this paper to cryo-EM in Theorem 4.3. We now state this result informally.

Theorem 1.1 (Informal theorem for cryo-EM). *In the cryo-EM model (1.3) (described in detail in Section 4.1), a generic K -sparse function $f \in V$ is uniquely determined by the second moment for $K \lesssim N/3$, where $N = \dim V$.*

Theorem 1.1 implies that sparse structures can be recovered, in the high noise regime, with only $n = \omega(\sigma^4)$ observations, improving upon $n = \omega(\sigma^6)$ for generic structures [8]. Figure 3 shows the distribution of wavelet coefficients (a standard choice of basis in many signal processing applications [63]) of a few molecular structures. Evidently, less than 1/3 of the coefficients capture almost all the energy of the volumes, suggesting that the bound of Theorem 1.1 is reasonable for typical molecular structures.

A recent paper [24] showed that a structure composed of ideal point masses (possibly convolved with a kernel with a non-vanishing Fourier transform) can be recovered from the second moment. However, the technique of [24] is tailored for this specific model. The same paper also suggests to recover a 3-D structure from the second moment based on a sparse expansion in a wavelet basis. Importantly, since our results hold for a generic choice of basis, it is not necessarily true for any specific choice, such as a wavelet basis.

Crystallographic phase retrieval. The second moment of the MRA model where random elements of the group of circular shifts \mathbb{Z}_N act on real signals in \mathbb{R}^N , is equivalent to the absolute values of the Fourier transform of the signal, known as the power spectrum. Recovering a signal from its power spectrum is called the phase retrieval problem and it has numerous applications in signal processing; see recent surveys and references therein [76, 15, 46, 20].

Recovering a sparse signal from the power spectrum is the main computational challenge in X-ray crystallography: a leading method for elucidating the atomic structure of molecules. This is by far the most important phase retrieval application. We discuss this problem in detail in Section 5. Our main result regarding the crystallographic phase retrieval problem states that a K -sparse signal $f \in \mathbb{R}^N$ with known support under a generic basis can be recovered from its power spectrum, up to a global phase, as long as $K \leq N/2$.

Organization of the paper The rest of the paper is organized as follows. Section 2 formulates the second moment of the MRA model (1.1) and shows that it determines the signal up to a set of unitary matrices. The section also provides several examples. Section 3 derives a bound on the sparsity level that allows unique recovery from the second moment (Theorem 3.1) in terms of the dimension and multiplicity of the irreducible representations, and provides examples. Section 4 focuses on cryo-EM: the main motivation of this paper. We formulate the cryo-EM model in detail, derive explicitly the ambiguities of the second moment, and deduce sparsity conditions allowing unique recovery (Theorem 4.3).

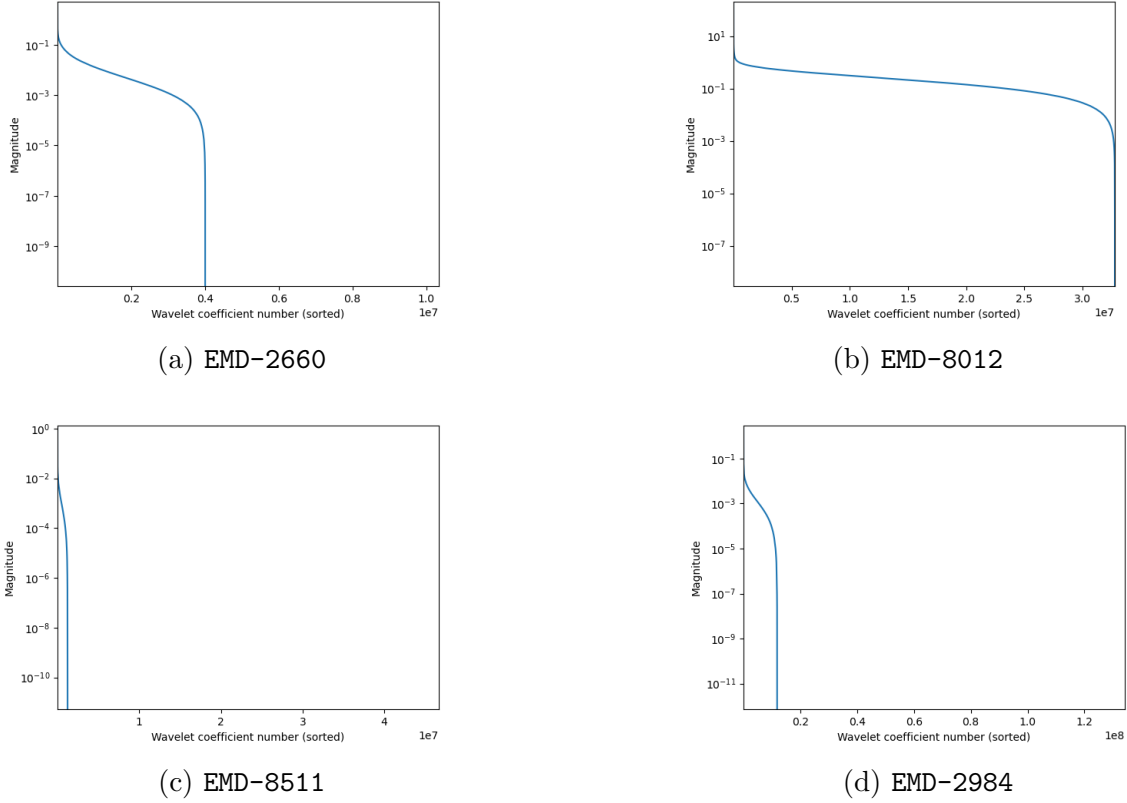


Figure 3: The sorted wavelet coefficients of cryo-EM structures whose experimental images are presented in Figure 2. The structures were downloaded from the Electron Microscopy Data Bank (EMDB) <https://www.ebi.ac.uk/emdb>. The structures were expanded using Haar wavelets, where the number of coefficients is approximately the same as the number of voxels. Besides EMD-8012, all the volumes energy (i.e., the squared norm of the coefficients) is captured by less than one third of the coefficients, which is the bound of Theorem 1.1. For EMD-8012, the same fraction of wavelet coefficients captures more than 91% of its energy.

Section 5 discusses the crystallographic phase retrieval problem. Section 6 concludes this work, and delineates future research directions. Appendix A provides necessary background in representation theory.

2 The second moment and symmetries

This section lays out the mathematical background for the second moments of the MRA model (1.1) for a compact group G acting on an N -dimensional real or complex vector space V . Following standard terminology, we refer to a vector space V equipped with an action of a group G as a *representation* of G . Our goal is to use methods from the representation theory of compact groups to understand the information obtained from the second moment. In Appendix A, we provide a necessary background in representation theory.

Any representation of a compact group is *unitary*. This means that elements of G act

on V as unitary transformations. In particular, the action of the group preserves the chosen Hermitian inner product. If V is a real vector space, then the action G is *orthogonal*, meaning that elements of G act by orthogonal transformations.

Let $\mathbb{K} = \mathbb{R}$ or $\mathbb{K} = \mathbb{C}$ be the field. Assuming that the distribution on the group G is uniform (Haar), then a choice of basis for an N -dimensional representation $V = \mathbb{K}^N$ expresses the second moment as a function $\mathbb{K}^N \rightarrow \mathbb{K}^{N^2}$ given by the formula

$$f \mapsto \int_G (g \cdot f)(g \cdot f)^* dg, \quad (2.1)$$

where $\mathbb{K}^{N^2} = \text{Hom}(V, V)$ is the vector space of linear transformations $V \rightarrow V$. The vector f is viewed as column vector so $(g \cdot f)(g \cdot f)^*$ is an $N \times N$, rank-one Hermitian matrix.

The second moment can also be defined without the use of coordinates, using tensor notation, as a map $V \rightarrow V \otimes V^*$,

$$f \mapsto \int_G (g \cdot f) \otimes \overline{(g \cdot f)} dg. \quad (2.2)$$

We will use both (2.1) and (2.2) interchangeably. The reason that these formulations are equivalent is that there is isomorphism of representations $V \otimes V^* \rightarrow \text{Hom}(V, V)$ as discussed in Appendix A.4. If we choose an orthonormal basis for V , then the tensor $f_1 \otimes \overline{f_2}$ corresponds to the matrix $f_1 f_2^*$.

Ultimately, we will view elements of V as functions $D \rightarrow \mathbb{C}$, where D is some domain on which G acts. For example, in cryo-EM $G = SO(3)$, and V is the subspace of $L^2(\mathbb{C}^3)$ consisting of the Fourier transforms of real-valued functions in $L^2(\mathbb{R}^3)$; this problem is discussed in detail in Section 4. The second moment of a function $f : D \rightarrow \mathbb{C}$ can be viewed as the function $m_f^2 : D \times D \rightarrow \mathbb{C}$, where

$$m_f^2(x_1, x_2) = \int_G (g \cdot f(x_1)) \overline{(g \cdot f(x_2))} dg, \quad (2.3)$$

where $g \cdot f : D \rightarrow \mathbb{C}$ is defined by $gf(x) = f(g^{-1}x)$.

2.1 The second moment of an irreducible representation of G

Recall that a representation is *irreducible* if it has no non-zero proper G -invariant subspaces. If the representation V is irreducible, then the following proposition shows that the second moment gives very little information about a vector $f \in V$.

Proposition 2.1. *Let V be an N -dimensional irreducible unitary representation of a compact group G and identify V with \mathbb{C}^N via a choice of orthonormal basis f_1, \dots, f_N of V . Then, as a map $\mathbb{C}^N \rightarrow \mathbb{C}^{N^2}$, the second moment is given by the formula*

$$f \mapsto |f|^2 I_N, \quad (2.4)$$

where I_N is the $N \times N$ identity matrix. In tensor notation, the second moment is the map $V \mapsto V \otimes V^*$ given by

$$f \mapsto |f|^2 \sum_{i=1}^N f_i \otimes \overline{f_i}. \quad (2.5)$$

Proof. If we identify the Hermitian matrix $m_f^2 = \int_G (g \cdot v)(g \cdot v)^* dg$ as giving a linear transformation $V \rightarrow V$, then the second moment defines a map $V \rightarrow \text{Hom}(V, V)$, where $\text{Hom}(V, V)$ is the group of linear transformations $V \rightarrow V$. Since the second moment is by definition invariant under the action of G on V (i.e., f and $g \cdot f$ both yield the matrix m_f^2), the matrix m_f^2 defines a G -invariant linear transformation on V . However since V is irreducible, by Schur's Lemma (Lemma A.3), any G -invariant linear transformation $V \rightarrow V$ is a scalar multiple of the identity. Since the map $f \mapsto m_f^2$ has the property that $m_{\lambda f} = |\lambda|^2 m_f$, we can after normalizing assume that the second moment is the map $f \mapsto |f|^2 I_N$.

The formula (2.5) is equivalent to the first formula because under the identification of $V \otimes V^*$ with $\text{Hom}(V, V) = \mathbb{K}^{N^2}$, the tensor $\sum_{i=1}^N f_i \otimes \bar{f}_i$ corresponds to the identity matrix. \square

2.2 The second moment for multiple copies of an irreducible representation

The following discussion is motivated by the situation in cryo-EM, where we view \mathbb{R}^3 as a collection of spherical shells. Thus, $\text{SO}(3)$ acting on $L^2(\mathbb{R}^3)$ implies taking a number of copies of $L^2(S^2)$. This is a standard model in cryo-EM, and is introduced in detail in Section 4.

Consider the case where the representation V decomposes as the direct sum of R copies of a single irreducible representation V_0 . In other words, there is a G -invariant isomorphism $V \simeq V_0^{\oplus R}$. This means that any vector $f \in V$ can be decomposed uniquely as $f = f[1] + \dots + f[R]$, with $f[r]$ in the r -th copy of V_0 . The summands are invariant under the action of G so $(g \cdot f)[r] = g \cdot f[r]$.

Since V decomposes as the sum $V_0^{\oplus R}$, the tensor product $V \otimes V^*$ decomposes as the sum of tensor products $\oplus_{i,j=1}^R V_0[i] \otimes V_0^*[j]$, where $V_0[r]$ indicates the r -th copy of V_0 in the decomposition of V . In particular, using tensor notation for the second moment, we can decompose

$$m_f^2 = \int_G (g \cdot f) \otimes \overline{(g \cdot f)} dg = \sum_{i,j=1}^R m_f^2[i, j], \quad (2.6)$$

where

$$m_f^2[i, j] = \int_G (g \cdot f[i]) \otimes \overline{(g \cdot f[j])} dg \in V_0[i] \otimes V_0^*[j], \quad (2.7)$$

is the component in the (i, j) -th summand of the tensor product $V \otimes V^*$. Each of the summands in (2.7) defines a G -invariant linear transformation $V_0[i] \rightarrow V_0[j]$.

Let $N_0 = \dim V_0$. For suitable orthonormal bases $f_1[i], \dots, f_{N_0}[i]$ and $f_1[j], \dots, f_{N_0}[j]$ of $V_0[i]$ and $V_0[j]$, respectively, Schur's Lemma implies that

$$m_f^2[i, j] = \int_G (g \cdot f[i]) \otimes \overline{(g \cdot f[j])} dg = \langle f[i], f[j] \rangle \left(\sum_{k=1}^{N_0} f_k[i] \otimes \overline{f_k[j]} \right).$$

To put this more directly, if we view an element of $V = V_0^{\oplus R}$ as an R -tuple $f[1], \dots, f[R]$ of elements of V_0 , then the second moment determines all pairwise inner products $\langle f[i], f[j] \rangle$. Equivalently, if we consider the vectors $f[1], \dots, f[R]$ as the column vectors of an $N_0 \times R$ matrix A , then the second moment determines the $R \times R$ Hermitian matrix $A^* A$.

Remark 2.2. Note that the vectors $f[1], \dots, f[R] \in V_0$ are determined from their pairwise inner products up to the action of the unitary group $U(N_0)$, parameterizing the isometries of V_0 . If, as will be the case for cryo-EM, we know that each $f[r]$ lies in a conjugation invariant subspace of V (for example, it is the Fourier transform of a real vector), then we can determine each $f[r]$ up to the action of a subgroup of $U(N_0)$ isomorphic to the real orthogonal group $O(N_0)$.

2.3 The second moment of a general finite dimensional representation and its group of ambiguities

A general finite dimensional representation of a compact group can be decomposed as

$$V = \bigoplus_{\ell=1}^L V_{\ell}^{\oplus R_{\ell}}, \quad (2.8)$$

with the V_{ℓ} are distinct (non-isomorphic) irreducible representations of G of dimension N_{ℓ} . An element of $f \in V$ has a unique G -invariant decomposition as a sum

$$f = \sum_{\ell=1}^L \sum_{i=1}^{R_{\ell}} f_{\ell}[i], \quad (2.9)$$

where $f_{\ell}[i]$ is in the i -th copy of the irreducible representation V_{ℓ} . In this case, the second moment decomposes as a sum of tensors $\int_G (g \cdot f_{\ell}[i]) \otimes \overline{(g \cdot f_m[j])} dg$. Each of these tensors determines a G -invariant map $V_{\ell}[i] \rightarrow V_m[j]$. Since $V_{\ell}[i]$ and $V_m[j]$ are non-isomorphic irreducible representations, Schur's Lemma implies that there are no non-zero G -invariant linear transformations $V_{\ell}[i] \rightarrow V_m[j]$ for $\ell \neq m$. In other words, we have a generalized orthogonality relation that the tensors $\int_G (g \cdot f_{\ell}[i]) \otimes \overline{(g \cdot f_m[j])} dg$ are zero if $\ell \neq m$ for all i, j .

Hence, the second moment decomposes as a sum

$$m_f^2 = \sum_{\ell=1}^L \sum_{i,j=1}^{R_{\ell}} \langle f_{\ell}[i], f_{\ell}[j] \rangle \left(\sum_{k=1}^{N_{\ell}} f_{k,\ell}[i] \otimes \overline{f_{k,\ell}[j]} \right), \quad (2.10)$$

where the vectors $f_{1,\ell}[i], \dots, f_{N_{\ell},\ell}[i]$ form an orthonormal basis for the i -th copy of the ℓ -th irreducible representation V_{ℓ} .

2.3.1 Functional representation of the second moment

If, as will be the case for our model of cryo-EM, we view the elements of V as functions $f: D \rightarrow \mathbb{C}$, then we can reformulate (2.10) as follows. Suppose that $f_{1,\ell}[i], \dots, f_{N_{\ell},\ell}[i]$ are functions $D \rightarrow \mathbb{C}$ which form an orthonormal basis for the i -th copy of the ℓ -th irreducible representation V_{ℓ} . If we expand $f_{\ell}[i] = \sum_{m=1}^{N_{\ell}} A_{\ell}^m[i] f_{m,\ell}[i]$, then the second moment realized as a function $D \times D \rightarrow \mathbb{C}$ is expanded as

$$m_f^2(x_1, x_2) = \sum_{\ell=1}^L \sum_{i,j=1}^{R_{\ell}} \left(\sum_{m=1}^{N_{\ell}} A_{\ell}^m[i] \overline{A_{\ell}^m[j]} \right) \left(\sum_{k=1}^{N_{\ell}} f_{k,\ell}[i](x_1) \overline{f_{k,\ell}[j](x_2)} \right), \quad (2.11)$$

where x_1, x_2 are, respectively, the variables on the first and second copies of D respectively.

2.3.2 The group of ambiguities

The main result of this section is a characterization of the group of ambiguities of the second moment. Later on, we provide a few explicit examples.

Theorem 2.3. *If V decomposes as a sum of irreducible representations $V = \bigoplus_{\ell=1}^L V_{\ell}^{R_{\ell}}$, where $\dim V_{\ell} = N_{\ell}$, then a vector $f \in V$ is determined from the second moment up to the action of the ambiguity group $H = \prod_{\ell=1}^L U(N_{\ell})$.*

Proof. If we decompose a vector $f \in V$ as in (2.9), then the second moment (2.10) determines the inner products $\langle f_{\ell}[i], f_{\ell}[j] \rangle$ for all $\ell = 1, \dots, L$ and $i, j \in 1, \dots, R_{\ell}$.

For a general representation, an element of V can be represented by an L -tuple (A_1, \dots, A_L) , where A_{ℓ} is an $N_{\ell} \times R_{\ell}$ complex matrix corresponding to an element in the summand $V_{\ell}^{\oplus R_{\ell}}$. The second moment determines the L -tuple of $R_{\ell} \times R_{\ell}$ Hermitian matrices $(A_1^* A_1, \dots, A_L^* A_L)$. In particular, a vector f is determined from the second moment up to the action of the product of unitary groups $\prod_{\ell=1}^L U(N_{\ell})$. \square

Remark 2.4 (Parameter counting). Since each unitary matrix is determined by N_{ℓ}^2 real parameters, the ambiguity group is of dimension $N_H = \sum_{\ell=1}^L N_{\ell}^2$. If the ambiguity group is isomorphic to the real orthogonal groups, as in cryo-EM (see Remark 2.2), then the ambiguity group is of dimension $N_H = \sum_{\ell=1}^L N_{\ell}(N_{\ell} - 1)/2$.

Remark 2.5. Note that the total dimension of the ambiguity group of the second moment does not depend on the multiplicities R_{ℓ} . In particular, the ratio of the dimensions is

$$\frac{N_H}{N} = \frac{\sum_{\ell=1}^L N_{\ell}^2}{2 \sum_{\ell=1}^L R_{\ell} N_{\ell}}. \quad (2.12)$$

This implies that as the number of multiplicities increases, the proportional amount of information about the signal contained in the second moment increases as well.

2.4 Examples

2.4.1 The power spectrum

Consider the group $G = \mathbb{Z}_N$ acting on \mathbb{K}^N by cyclic shifts, where $\mathbb{K} = \mathbb{R}$ or $\mathbb{K} = \mathbb{C}$. In the Fourier domain, the cyclic group $G = \mathbb{Z}_N$ acts by multiplication by roots of unity. In particular, we identify $\mathbb{Z}_N = \mu_N$, where μ_N is the N -th roots of unity. If $\omega \in \mu_N$, then

$$\omega \cdot (f[0], \dots, f[N-1]) = (f[0], \omega f[1], \dots, \omega^{N-1} f[N-1]). \quad (2.13)$$

The vector space \mathbb{C}^N with this action of μ_N decomposes as a sum of one-dimensional irreducible representations (namely, $N_{\ell} = R = 1$ so that $N = L$) $V_0 \oplus \dots \oplus V_{N-1}$, where $\omega \in \mu_N$ acts on V_i by $\omega \cdot f[i] = \omega^i f[i]$. The second moment of a vector $f \in \mathbb{C}^N$ in the Fourier domain is the power spectrum $(|f[0]|^2, \dots, |f[N-1]|^2)$. This determines the vector up to the action of the group $(S^1)^N$ since $U(1) = S^1$.

Recall that the image of \mathbb{R}^N under the discrete Fourier transform is the real subspace of \mathbb{C}^N given by the condition $f[N-i] = \overline{f[i]}$. Thus, if f is the Fourier transform of a real

vector, the ambiguity group must preserve the condition that $f[N-i] = \overline{f[i]}$ and is therefore the subgroup of

$$\{(\lambda_0, \dots, \lambda_{N-1} | \lambda_{N-n} = \lambda_n^{-1}) \subset (S^1)^N. \quad (2.14)$$

Recovering a signal from its power spectrum is called the phase retrieval problem [76, 15, 46, 20]; see Section 5 for further discussion.

2.4.2 Dihedral MRA

Consider the action of the dihedral group $G = D_{2N}$ acting \mathbb{K}^N , where the rotation $r \in D_{2N}$ acts by cyclic shift and the reflection $s \in D_{2N}$ acts by $(s \cdot f)[i] = f[N-i]$. In the Fourier domain, $(s \cdot f)[i] = \overline{f[N-i]}$ and $(r \cdot f)[i] = \omega^i f[i]$ as in (2.13). In [21], it was shown that the orbit of a generic signal is determined uniquely from the second moment if the group elements are drawn from a non-uniform distribution over the dihedral group. Here, we consider a uniform (Haar) distribution of the group elements.

The vector space \mathbb{C}^N with this action of D_{2N} decomposes into a sum of one and two-dimensional irreducible representations, depending on the parity of N . If N is even, then

$$\mathbb{C}^N = V_0 \oplus V_1 \oplus \dots \oplus V_{N/2-1} \oplus V_{N/2},$$

where V_0 is the one dimensional subspace spanned by the vector $e_0 = (1, 0, \dots, 0)$, $V_{N/2}$ is spanned by the vector $e_{N/2}$, and for $1 \leq i \leq N/2-1$, V_i is the subspace spanned by $\{e_i, e_{N-i}\}$. Similarly, if N is odd, then

$$\mathbb{C}^N = V_0 \oplus V_1 \dots \oplus V_{(N-1)/2},$$

where again V_0 is spanned by e_0 and for $i \geq 1$ V_i is spanned by $\{e_i, e_{N-i}\}$.

Therefore, the second moment of a vector f in the Fourier domain determines the $N/2+1$ real numbers

$$(|f[0]|^2, |f[1]|^2 + |f[N-1]|^2, \dots, |f[N/2-1]|^2 + |f[N/2+1]|^2, |f[N/2]|^2)$$

if N is even, and the $N+1/2$ real numbers

$$(|f[0]|^2, |f[1]|^2 + |f[N-1]|^2, \dots, |f[(N-1)/2]|^2 + |f[(N+1)/2]|^2)$$

if N is odd. When $\mathbb{K} = \mathbb{C}$, this is less information than the power spectrum. When N is even, the ambiguity group is $S^1 \times U(2)^{N/2} \times S^1$ and when N is odd the ambiguity group is $S^1 \times U(2)^{(N-1)/2}$. However, if $\mathbb{K} = \mathbb{R}$ then the second moment gives the power spectrum because if f is the Fourier transform of a real vector then we have $|f[i]| = |f[N-i]|$. In this case, the ambiguity group is $\pm 1 \times O(2)^{N/2} \times \pm 1$ if N is even and if N is odd then it is $\pm 1 \times O(2)^{(N-1)/2}$. These groups are isomorphic to the subgroups of $(S^1)^N$ considered in (2.14).

2.4.3 MRA with rotated images

In this model the Fourier transform of an image is represented as a radially discretized band limited function on \mathbb{C}^2 . That is, our function f is expressed as $f = (f[1], \dots, f[R])$, where

$$f[r](\theta) = \sum_{k=-L}^L a_{k,r} e^{i\theta k}, \quad \theta \in [0, 2\pi), \quad (2.15)$$

for some bandlimit L and R radial samples. The action of a rotation S^1 on the image is given by

$$e^{\iota\alpha} \cdot f[r](\theta) = \sum_{k=-L}^L a_{k,r} e^{\iota(\theta-\alpha)k} = \sum_{k=-L}^L a_{k,r} e^{-\iota\alpha k} e^{\iota\theta k}.$$

With this action, the parameter space of two dimensional images is the S^1 -representation $V = V_{-L}^R \oplus \dots \oplus V_L^R$, where V_k is the one-dimensional representation of S^1 , where $e^{\iota\alpha} \in S^1$ acts with weight $-k$. The (r_1, r_2) component of the second moment equals

$$\begin{aligned} m_f^2[r_1, r_2](\theta_1, \theta_2) &= \int_{\alpha} e^{-\iota\alpha} f[r_1](\theta_1) \overline{e^{-\iota\alpha} f[r_2](\theta_2)} d\alpha \\ &= \int_{\alpha} \sum_{k_1=-L}^L a_{k_1, r_1} e^{\iota(\theta_1-\alpha)k_1} \sum_{k_2=-L}^L \overline{a_{k_2, r_2}} e^{-\iota(\theta_2-\alpha)k_2} d\alpha \\ &= \sum_{k=-L}^L a_{k, r_1} \overline{a_{k, r_2}} e^{\iota(\theta_1-\theta_2)k} \\ &= \sum_{k=-L}^L a_{k, r_1} \overline{a_{k, r_2}} e^{\iota\Delta\theta k} \\ &= m_f^2[r_1, r_2](\Delta\theta), \end{aligned} \tag{2.16}$$

where $\Delta\theta := \theta_1 - \theta_2$. Following our previous discussion, a function $f \in V$ is determined by a $(2L+1)$ -tuple of $1 \times R$ matrices (A_{-L}, \dots, A_L) , where $A_k = (a_{k,1}, \dots, a_{k,R})^T$. The second moment computes the $(2L+1)$ -tuple of rank-one $R \times R$ matrices $(A_{-L}^* A_{-L}, \dots, A_L^* A_L)$. Since each irreducible summand in the representation V has dimension one (namely, $N_\ell = 1$ for all ℓ), the ambiguity group of the second moment for the rotated images problem is $(S^1)^{2L+1}$. If we assume that the function f is the Fourier transform of a real valued function, then $a_{k,r} = \overline{a_{-k,r}}$ and the ambiguity group is $O(2)^L \times \pm 1$.

2.4.4 Two-dimensional tomography from unknown random projections

The problem of recovering a two-dimensional image from its tomographic projections is a classical problem in computerized tomography (CT) imaging [64]. However, in some cases, the viewing angles are unknown and may be considered random. Due to the Fourier Slice Theorem, this is equivalent to randomly rotating the image, and then acquiring a single one-dimensional line of its Fourier transform. While generally an image cannot be recovered from such random projections (in contrast to the three-dimensional counterpart (1.3), where recovery is theoretically possible based on the common-lines property [82, 77]), it was shown that unique recovery, up to rotation, requires rather mild conditions [13]. Different algorithms were later developed, see for example [34, 84, 91].

In this model, we compute the second moment of the Fourier transform of the image after tomographic projection to a line. In other words, we compute the integral

$$\int_{S^1} T e^{\iota\alpha} \cdot f[r_1](\theta_1) \overline{T e^{\iota\alpha} \cdot f[r_2](\theta_2)} d\alpha,$$

where T is the tomographic projection to the line $\theta = 0$ (the two-dimensional counterpart of (1.4)). In this case, we obtain a function only of r_1, r_2 (compare with (2.16))

$$m_f^2[r_1, r_2] = \sum_{k=-L}^L a_{k,r_1} \overline{a_{k,r_2}}.$$

If we view the $(2L+1)$ -tuple of $1 \times R$ matrices (A_{-L}, \dots, A_L) as a single $(2L+1) \times R$ -matrix A , then the projected second moment determines the Hermitian matrix A^*A . Equivalently, an element of V is determined by R vectors in \mathbb{C}^{2L+1} and the projected second moment determines all pairwise inner products of these vectors. In this case, the ambiguity group is $U(2L+1)$ (or $O(2L+1)$ if the image is the Fourier transform of a real-valued function) compared to $(S^1)^{2L+1}$ in the unprojected case (respectively, $O(2)^L \times \pm 1$).

3 Retrieving the unitary matrix ambiguities for sparse signals

In the previous section, we have shown that it is generally impossible to recover a vector f in a representation V of a compact group G from its second moment due to the large group of ambiguities. To resolve these ambiguities and recover the signal in either the MRA (1.1) or cryo-EM (1.3) models, we need a prior on the sought signal. In this work, we assume that the signal is sparse in some basis. This assumption has been studied and harnessed in the MRA [25, 44] and cryo-EM literature [24, 87, 50, 54, 40, 90]. In this section, we derive bounds on the sparsity level that allows retrieving the missing unitary matrices, as a function of the dimensions and multiplicities of the irreducible representations. We also provide a couple of examples, and leave more detailed discussions on cryo-EM and phase retrieval to, respectively, Section 4 and Section 5.

3.1 Sparsity conditions

Let V be an N -dimensional vector space. The notion of sparsity depends on the choice of an orthonormal basis $\mathcal{V} = \{f_1, \dots, f_N\}$. A vector $f \in V$ is K -sparse with respect to this ordered basis if f is a linear combination of at most K elements of this basis. The set of K -sparse vectors with respect to an ordered basis \mathcal{V} is the union of $\binom{N}{K}$ linear subspaces $\mathbb{L}_S(\mathcal{V})$, where $\mathbb{L}_S(\mathcal{V})$ is the subspace spanned by the vectors $\{f_i\}_{i \in S}$ and S is a K -element subset of $[1, N]$.

Let

$$V = \oplus_{\ell=1}^L V_\ell^{R_\ell}, \quad (3.1)$$

be a representation of a compact group G , where $\dim V_\ell = N_\ell$. Let $H = \prod_{\ell=1}^L U(N_\ell)$ be the ambiguity group of the second moment (see Theorem 2.3).

The main result of this section is the following.

Theorem 3.1. *Let V be a representation as in (3.1), let $N = \sum_{\ell=1}^L N_\ell R_\ell$ be its total dimension and let $M = \sum_{\ell=1}^L \min(N_\ell R_\ell, N_\ell^2)$. Then, for a generic choice of orthonormal basis*

\mathcal{V} , a generic K -sparse vector $f \in V$ with $K \leq N - M$ is uniquely determined by its second moment, up to a global phase.

Remark 3.2 (Frames). Recall that a collection \mathcal{F} of vectors in a finite-dimensional vector space V is a *frame* if the vectors span V . The methods used to prove Theorem 3.1 can also be used to prove a corresponding result where orthonormal bases are replaced by arbitrary frames. The only difference between working with frames instead of bases is that definition of a vector being sparse with respect to an ordered frame is more subtle. The reason is that for a generic frame \mathcal{F} any N -element subset consists of linearly independent vectors, so any $f \in V$ which has zero frame coefficients with respect to N elements in \mathcal{F} must necessarily be zero. In particular, if we work with frames, then the condition that a vector is K -sparse should be replaced by the condition that at least $N - K$ of the frame coefficients are zero. Otherwise, the statements and proofs remain the same.

3.1.1 Strategy and remarks on the proof

The proof of Theorem 3.1 involves a number of steps. Suppose that \mathcal{V} is a generic orthonormal basis and consider the set of vectors which are K -sparse with respect to \mathcal{V} . The set of such vectors form the union of $\binom{N}{K}$ K -dimensional linear subspaces of V . The strategy of the proof is to show that with bounds on K given in the Theorem 3.1, the following is true: if f is a generic K -sparse vector with respect to the orthonormal basis \mathcal{V} , the only vectors in the H -orbit of f which are also K -sparse are of the form $e^{i\alpha}f$.

To prove this result, we will actually prove something stronger. Rather than consider the H -orbit of a vector f , we will consider the linear span of its orbit and prove that the only K -sparse vectors in the linear span of the orbit of f are scalar multiples of f . The advantage of working with the linear span is that we can use techniques from linear algebra to understand when a linear subspace (the linear span of our orbit) intersects the $\binom{N}{K}$ K -dimensional linear subspaces consisting of vectors which are K -sparse with respect to the given orthonormal basis \mathcal{V} .

The price we pay for working with the linear span of an orbit instead of directly working with the orbit is that if the H orbit of f has real dimension M , then its linear span is a complex linear subspace of complex dimension M or equivalently real dimension $2M$ (see Proposition 3.3). As a result, the sparseness bound we obtain may not be optimal. However, when $\dim H \ll \dim V$, as is the case in cryo-EM, this gap is not significant.

Finally, we remark that for the general MRA problem with group G (1.1), we can at best recover the G -orbit of a vector f from its moments. However, by imposing the prior condition that the vector is sparse with respect to a given basis we have the possibility of recovering a vector up to a global phase. The reason is that for a general orthonormal basis \mathcal{V} of V , the sparse vectors are not invariant under the action of G .

3.2 Proof of Theorem 3.1

Let H be a group acting on a vector space V and $f \in V$ any vector. We denote by \mathbb{L}_f the *linear span* of the H -orbit Hf . By definition $\mathbb{L}_f = \{\sum a_i(h_i \cdot f) | a_i \in \mathbb{C}, h_i \in H\}$ and it is the smallest linear subspace containing the orbit Hf .

Let $V = \bigoplus_{\ell=1}^L V_\ell^{R_\ell}$ be a unitary representation of a compact group G and let $H = \prod_{\ell=1}^L U(N_\ell)$. Given a vector $f \in V$, we can write $f = \sum_{\ell=1}^L \sum_{r=1}^{R_\ell} f_\ell[r]$, where $f_\ell[r]$ is in the r -th copy of the irreducible representation V_ℓ . As above, we can view our vector f as an L -tuple (A_1, \dots, A_L) of $N_\ell \times R_\ell$ matrices with $A_\ell = (f_\ell[1])^T, \dots, (f_\ell[R_\ell])^T$. Viewing $V_\ell^{R_\ell}$ as the vector space of $N_\ell \times R_\ell$ matrices, the linear span \mathbb{L}_f of the orbit Hf is the product of the $U(N_\ell)$ orbits of the matrices A_ℓ , where elements of $U(N_\ell)$ acts on A_ℓ by left multiplication.

Proposition 3.3. *Let $V = \bigoplus_{\ell=1}^L V_\ell^{R_\ell}$ be a unitary representation of a compact group G and let $H = \prod_{\ell=1}^L U(N_\ell)$. If $f \in V$ is represented by an L -tuple (A_1, \dots, A_L) of $N_\ell \times R_\ell$ matrices, then*

$$\dim_{\mathbb{C}} \mathbb{L}_f = \sum_{\ell=1}^L (\text{rank } A_\ell) N_\ell,$$

where $\dim_{\mathbb{C}}$ denotes the dimension of \mathbb{L}_f as a complex vector space. In particular,

$$\dim_{\mathbb{C}} \mathbb{L}_f \leq \sum_{\ell=1}^L M_\ell,$$

where $M_\ell = \min(N_\ell R_\ell, N_\ell^2)$.

Proof. Since the linear span of the H -orbit of $f = (A_1, \dots, A_L)$ is the product of the linear spans of the $U(N_\ell)$ -orbits of the matrices A_ℓ , it suffices to prove that the linear span of the $U(N_\ell)$ -orbit of the matrix A_ℓ in $V_\ell^{R_\ell}$ has dimension $(\text{rank } A_\ell) N_\ell$.

Let $r_\ell = \text{rank } A_\ell$ and to simplify notation assume that the first r_ℓ columns $f_\ell[1]^T, \dots, f_\ell[r_\ell]^T$ of A_ℓ are linearly independent. Since $\text{rank } A_\ell = r_\ell$, for $r > r_\ell$ there are unique scalars $b_{1,r}, \dots, b_{r_\ell,r}$ such that $f_\ell[r] = \sum_{i=1}^{r_\ell} b_{i,r} f_\ell[i]$.

Let \mathbb{L}_{A_ℓ} be the $r_\ell N_\ell$ -dimensional linear subspace of $V_\ell^{R_\ell}$ consisting of $N_\ell \times R_\ell$ matrices B such that for $r > r_\ell$, $B_r = \sum_{i=1}^{r_\ell} b_{i,r} B_i$, where B_i denotes the i -th column of the matrix B . Since $U(N_\ell)$ acts linearly, the linear relations on the columns of A_ℓ are preserved by the action of $U(N_\ell)$, so the linear span of $U(N_\ell)A_\ell$ lies in the subspace \mathbb{L}_{A_ℓ} . Conversely, we note that the linear span of $U(N_\ell)A_\ell$ contains the open set $\mathbb{L}_{A_\ell}^o$ of \mathbb{L}_{A_ℓ} , parameterizing matrices whose first r_ℓ columns are linearly independent. The reason this holds is because any invertible $N_\ell \times N_\ell$ matrix is a linear combination of unitary matrices and any element of $\mathbb{L}_{A_\ell}^o$ can be obtained by applying some invertible matrix to A_ℓ . \square

Remark 3.4. Note that the real dimension of the $U(N_\ell)$ -orbit of the matrix A_ℓ considered in the proof of Proposition 3.3 has real dimension $r_\ell N_\ell$. It follows that for any vector $f \in V$, $\dim_{\mathbb{C}} \mathbb{L}_f = \dim_{\mathbb{R}} Hf$. In particular, the real dimension of \mathbb{L}_f is twice the real dimension of the orbit Hf .

Proposition 3.5. *Let $f \in V$ be any non-zero vector and let \mathbb{L}_f be the linear span of its orbit under H . Let $\mathbb{L}_{\{1, \dots, K\}}(\mathcal{V})$ denote the linear subspace spanned by the first K vectors of the ordered basis \mathcal{V} . Then, if $K \leq N - M$, there exists an orthonormal basis \mathcal{V} for V such that:*

1. \mathbb{L}_f intersects $\mathbb{L}_{\{1, \dots, K\}}(\mathcal{V})$ in the line spanned by f ;
2. $\mathbb{L}_f \cap \mathbb{L}_S(\mathcal{V}) = \{0\}$ if $S \neq \{1, \dots, K\}$.

To prove Proposition 3.5 we need to introduce some notation and prove a lemma.

Fix an orthonormal basis e_1, \dots, e_N of a Hermitian vector space V of dimension N . For $S \subset [1, N]$ with $|S| = K$, let $\mathbb{L}_S = \text{span}\{e_i\}_{i \in S}$ and \mathbb{L}_S^* be the open subset of \mathbb{L}_S of vectors whose expansion with respect to the basis $\{e_i\}_{i \in S}$ have all non-zero coordinates. In other words, $\mathbb{L}_S^* = \mathbb{L}_S \setminus (\bigcup_{S' \neq S} \mathbb{L}_{S'})$.

For a given vector $w \in V$, let $\text{Gr}_w(M, V)$ be the subvariety of the Grassmannian of M -dimensional linear subspaces of V that contain w .

Lemma 3.6. *If $K \leq N - M$, then for any vector $w \in \mathbb{L}_{\{1, \dots, K\}}^*$ the generic M -dimensional linear subspace $\mathbb{L} \in \text{Gr}_w(M, V)$ satisfies the following conditions:*

1. $\mathbb{L} \cap \mathbb{L}_{\{1, \dots, K\}}$ is the line spanned by w ;
2. $\mathbb{L} \cap \mathbb{L}_S = \{0\}$ for $S \neq \{1, \dots, K\}$ and $|S| = K$.

Proof of Lemma 3.6. The subset of $\text{Gr}_w(M, V)$ parameterizing linear subspaces intersecting $\mathbb{L}_{\{1, \dots, K\}}$ in dimension greater than one is locally defined by a polynomial equation and therefore a proper algebraic subset. Likewise, for any $S \neq \{1, \dots, K\}$ the subset of $\text{Gr}_w(M, V)$ parameterizing linear subspace \mathbb{L} such that $\mathbb{L} \cap \mathbb{L}_S \neq \{0\}$ is also defined by a polynomial equation, and thus is again a proper algebraic subset. In particular, the set of $\mathbb{L} \in \text{Gr}_w(M, V)$ which do not satisfy conditions (1) and (2) lie in a proper algebraic subset of $\text{Gr}_w(M, V)$. Therefore, the generic subspace $\mathbb{L} \in \text{Gr}_w(M, V)$ satisfies conditions (1) and (2). \square

Proof of Proposition 3.5. Choose a fixed orthonormal basis $\{e_1, \dots, e_N\}$ and let (\mathbb{L}, w) be an M -dimensional linear subspace and vector satisfying the conclusions (1) and (2) of Lemma 3.6. If we choose w so that $|w| = |f|$, then we can find a rotation $g \in U(N)$ such that $g \cdot (\mathbb{L}, w) = (\mathbb{L}_f, f)$. The orthonormal basis $\{v_i = g \cdot e_i\}_{i=1, \dots, N}$ satisfies conditions (1) and (2) of the proposition. \square

We can conclude the proof of Theorem 3.1 with the following proposition.

Proposition 3.7. *Let \mathcal{V} be an ordered orthonormal basis for V and assume that there is a non-zero vector $f_0 \in L_{\{1, \dots, K\}}(\mathcal{V})$ such that $\dim \mathbb{L}_{f_0} \cap \mathbb{L}_{\{1, \dots, K\}}(\mathcal{V}) = 1$ and $\mathbb{L}_{f_0} \cap \mathbb{L}_S(\mathcal{V}) = \{0\}$ for $S \neq \{1, \dots, K\}$. Then, for a generic $f \in L_{\{1, \dots, K\}}(\mathcal{V})$ the same property holds.*

Proof. Given an orthonormal basis \mathcal{V} , the set D of $f \in L_{\{1, \dots, K\}}(\mathcal{V})$ which satisfy the condition that $\dim \mathbb{L}_f \cap \mathbb{L}_{\{1, \dots, K\}}(\mathcal{V}) > 1$ or $\dim \mathbb{L}_f \cap \mathbb{L}_S(\mathcal{V}) > 0$ for $S \neq \{1, \dots, K\}$ is defined by polynomial equations. By hypothesis, we know that $D \neq L_{\{1, \dots, K\}}$ since $f_0 \notin D$ so its complement is necessarily Zariski dense. \square

3.3 Examples

3.3.1 MRA with rotated images model

Using Theorem 3.1 we can obtain sparsity bounds for recovering a generic image from its second moment as in Section 2.4.3.

Recall that in this model the Fourier transform of an image is represented as a radially discretized band-limited function on \mathbb{C}^2 , and the function f is determined by a $(2L+1)$ -tuple

(A_{-L}, \dots, A_L) vectors in \mathbb{C}^R , where L is the bandlimit and R is the number of radial samples. The ambiguity group is $H = (S^1)^{2L+1}$. In the notation of Theorem 3.1, we have $M_\ell = 1$ for $\ell = -L, \dots, L$. In particular, for any vector $f \in V$, $\dim \mathbb{L}_f \leq 2L+1$. Hence, by Theorem 3.1 we can conclude that if $K \leq \dim V - (2L+1)$, then for a generic orthonormal basis, a generic K -sparse vector can be recovered from its second moment. Since $\dim V = R(2L+1)$, if the number of radial samples $R \geq 2$, then the sparsity level required for signal recovery is $K \leq \frac{R-1}{R}N$, namely, linear in $\dim V$. If only one radial sample is taken ($R = 1$), then this problem reduces to the MRA model on the circle, which is equivalent to the Fourier phase retrieval problem [15].

3.3.2 Sparsity bounds for two-dimensional tomography from unknown random projections

Following the model of Section 2.4.4, the unknown image f is viewed as a $(2L+1) \times R$ matrix A and the projected second moment determines the matrix A^*A . Thus, the ambiguity group is $U(2L+1)$ (complex images) or $O(2L+1)$ (real images). The orbit of a generic signal f has dimension Mm where $M = \min(\dim V, (2L+1)^2)$. Since $\dim V = (2L+1)R$, we have $M = \min(R(2L+1), (2L+1)^2)$. In order to be able to recover sparse signals we need to take $R > (2L+1)$; i.e., the number of radial samples must exceed the number of frequencies. Specifically, Theorem 3.1 implies that for a generic ordered orthonormal basis \mathcal{V} we can recover K -sparse signals where $K = (R - (2L+1))(2L+1)$. In particular, if $R > p(2L+1)$ with $p > 1$, then a generic K -sparse signal is uniquely determined by its second moment if $K \leq \frac{p-1}{p}N$, where $N = \dim V$.

4 Application to cryo-EM

This section is devoted to the application of the results of Section 2 and Section 3 to single-particle cryo-EM: the main motivation of this work.

Recent technological breakthroughs in cryo-EM have sparked a revolution in structure biology—the field that studies the structure and dynamics of biological molecules—by recovering an abundance of new molecular structures at near-atomic resolution. In particular, cryo-EM allows recovering molecules that were notoriously difficult to crystallize (e.g., different types of membrane proteins), the sample preparation procedure is significantly simpler (compared to alternative technologies) and preserves the molecules in a near-physiological state, and it allows reconstructing multiple functional states.

In this section, we describe the mathematical model of cryo-EM in detail, formulate the ambiguities of recovering the three-dimensional structure from the second moment, and then derive the sparsity level that allows resolving these ambiguities based on Theorem 3.1.

4.1 Mathematical model

Let $L^2(\mathbb{R}^3)$ be Hilbert space of complex valued L^2 functions on \mathbb{R}^3 . The action of $SO(3)$ on \mathbb{R}^3 induces a corresponding action on $L^2(\mathbb{R}^3)$, which we view as an infinite-dimensional representation of $SO(3)$. In cryo-EM we are interested in the action of $SO(3)$ on the subspace

of $L^2(\mathbb{R}^3)$ corresponding to the Fourier transforms of real valued functions on \mathbb{R}^3 , representing the coulomb potential of an unknown molecular structure.

Using spherical coordinates (ρ, θ, ϕ) , we consider a finite dimensional approximation of $L^2(\mathbb{R}^3)$ by discretizing $f(\rho, \theta, \phi)$ with R samples r_1, \dots, r_R , of the radial coordinates and bandlimiting the corresponding spherical functions $f(r_i, \theta, \phi)$. This is a standard assumption in the cryo-EM literature, see for example [10]. Mathematically, this means that we approximate the infinite-dimensional representation $L^2(\mathbb{R}^3)$ with the finite dimensional representation $V = (\oplus_{\ell=0}^L V_\ell)^R$, where L is the bandlimit, and V_ℓ is the $(2\ell + 1)$ -dimensional irreducible representation of $SO(3)$, corresponding to harmonic polynomials of frequency ℓ . An orthonormal basis for V_ℓ is the set of spherical harmonic polynomials $\{Y_\ell^m(\theta, \phi)\}_{m=-\ell}^\ell$. We use the notation $Y_\ell^m[r]$ to consider the corresponding spherical harmonic as a basis vector for functions on the r -th spherical shell. The dimension of this representation is $R(L^2 + 2L + 1)$.

Viewing an element of V as a radially discretized function on \mathbb{R}^3 , we can view $f \in V$ as an R -tuple

$$f = (f[1], \dots, f[R]),$$

where $f[r] \in L^2(S^2)$ is an L -bandlimited function. Each $f[r]$ can be expanded in terms of the basis functions $Y_\ell^m(\theta, \varphi)$ as follows

$$f[r] = \sum_{\ell=0}^L \sum_{m=-\ell}^{\ell} A_\ell^m[r] Y_\ell^m. \quad (4.1)$$

Therefore, the problem of determining a structure reduces to determining the unknown coefficients $A_\ell^m[r]$ in (4.1).

Note that when f is the Fourier transform of a real valued function, the coefficients $A_\ell^m[r]$ are real for even ℓ and purely imaginary for odd ℓ [26].

4.2 The second moment of the cryo-EM model

In this section, we first formulate the second moment of the MRA model (1.1) for $G = SO(3)$ and functions of the form (4.1). Then, we show that this is equivalent to the second moment of the cryo-EM model (Lemma 4.1) and derive the ambiguity group of this model (Corollary 4.2).

Consider the MRA model with $G = SO(3)$ and functions of the form (4.1). Using the expansion from the previous section and the functional representation of the second moment (2.11), we can write

$$m_f^2 = \sum_{r_1, r_2=1}^R \sum_{\ell=0}^L \left(\sum_{m=-\ell}^{\ell} A_\ell^m[r_1] \overline{A_\ell^m[r_2]} \right) \sum_{m'=-\ell}^{\ell} Y_\ell^{m'}[r_1] \overline{Y_\ell^{m'}[r_2]}, \quad (4.2)$$

where the notation $Y_\ell^m[r]$ denotes the corresponding spherical harmonic in the r -th copy of $V_\ell \subset L^2(S^2)$. To simplify notation, set

$$B_\ell[r_1, r_2] = \sum_{m=-\ell}^{\ell} A_{\ell, m}[r_1] \overline{A_{\ell, m}[r_2]}. \quad (4.3)$$

This can be viewed as an inner product of the coefficient vector $(A_\ell^{-\ell}[r_1], \dots, A_\ell^\ell[r_1])$ from the r_1 -shell and the coefficient vector $(A_\ell^{-\ell}[r_2], \dots, A_\ell^\ell[r_2])$ from the r_2 shell. Let $A_\ell \in \mathbb{C}^{(2\ell+1) \times R}$ and $B_\ell \in \mathbb{C}^{R \times R}$ be matrices consisting of the coefficients

$$A_\ell = (A_\ell^m[r_i])_{m=-\ell, \dots, \ell, i=1, \dots, R},$$

and

$$B_\ell = (B_\ell[r_i, r_j])_{i, j=1, \dots, R}.$$

Then, the second moment determines the matrices

$$B_\ell = A_\ell^T A_\ell, \quad \ell = 0, \dots, L. \quad (4.4)$$

Remarkably, the tomographic projection operator (1.4) does not affect the second moment. Therefore, in the context of the second moment, we can treat cryo-EM as a special case of the MRA model (1.3), where G is the group of three-dimensional rotations $SO(3)$ and V is a discretization of $L^2(\mathbb{R}^3)$ as in (4.1). This fact has been recognized (implicitly) early on already by Zvi Kam [52]. For completeness, we prove the following lemma.

Lemma 4.1. *Assume a function of the form (4.1). Then, the second moment of the cryo-EM model (1.3) is the same as the second moment of the MRA model (1.1) with $G = SO(3)$. Namely, the tomographic projection operator in (1.3) does not affect the second moment.*

Proof. Consider the projected second moment of a function $f \in V$ for fixed (r_1, r_2) :

$$\begin{aligned} \int_{SO(3)} T(g \cdot f[r_1](\theta_1, \phi_2)) \overline{T(g \cdot f[r_2](\theta_2, \phi_2))} dg &= (T \times T) \int_{SO(3)} (g \cdot f[r_1](\theta_1, \phi_1)) \overline{(g \cdot f[r_2](\theta_2, \phi_2))} dg \\ &= (T \times T)(m_f^2[r_1, r_2](\theta_1, \phi_1, \theta_2, \phi_2)) \quad (4.5) \\ &= \sum_{\ell=0}^L B_\ell[r_1, r_2] \sum_{m=-\ell}^{\ell} Y_\ell^m(\pi/2, \varphi_1)[r_1] \overline{Y_\ell^m(\pi/2, \varphi_2)[r_2]}. \end{aligned}$$

Here, $T \times T$ is the product of tomographic projections so $(T \times T)f(\theta_1, \phi_1, \theta_2, \phi_2) = f(\pi/2, \phi_1, \pi/2, \phi_2)$. Note that the first equality holds because the linear operator T commutes with integration over the group $SO(3)$. Let P_ℓ be the Legendre polynomial of degree ℓ . Since, up to constants [6, Section 2.2],

$$\sum_{m=-\ell}^{\ell} Y_\ell^m(\pi/2, \varphi_1) \overline{Y_\ell^m(\pi/2, \varphi_2)} = P_\ell(\cos(\varphi_1 - \varphi_2)), \quad (4.6)$$

we have

$$\int_G T(g \cdot f[r_1]) \overline{T(g \cdot f[r_2])} dg = \sum_{\ell=0}^L B_\ell[r_1, r_2] P_\ell(\cos(\varphi_1 - \varphi_2)). \quad (4.7)$$

Since the Legendre polynomials are orthonormal functions of $\varphi = \varphi_1 - \varphi_2$, we can determine the coefficients $B_\ell[r_1, r_2]$ from (4.7). Thus we can conclude that no information is lost from the taking the projected second moment. \square

Corollary 4.2. Assume a function of the form

$$f[r] = \sum_{\ell=0}^L \sum_{m=-\ell}^{\ell} A_{\ell}^m[r] Y_{\ell}^m.$$

Then, the second moment of the cryo-EM model (1.3) is given by (4.4). Therefore, the second moment determines the coefficient matrices A_{ℓ} , $\ell = 0, \dots, L$ up to the action of the ambiguity group $\prod_{\ell=0}^L U(2\ell + 1)$. Moreover, if we consider functions $f[r]$ which are the Fourier transforms of real-valued functions on \mathbb{R}^3 (which is the scenario in cryo-EM), then the coefficients $A_{\ell}^m[r]$ are real for even ℓ and purely imaginary for odd ℓ [26], and the ambiguity group is $\prod_{\ell=0}^L O(2\ell + 1)$.

4.3 Recovery of sparse structures from the 2nd-moment

Based on Theorem 3.1, we now prove that in cryo-EM a K -sparse signal can be recovered from the second moment when $K \lesssim N/3$.

Theorem 4.3. Assume a function of the form (4.1), where the number of shells satisfies $R \geq 2L + 1$. Let $V = \oplus_{\ell=0}^L V_{\ell}^R$ and let $N = \dim V$. Then, if

$$\frac{K}{N} \leq \frac{2/3L^3 + L^2 + L/3}{2L^3 + 5L^2 + 4L + 1} \approx \frac{1}{3},$$

then for a generic choice of orthonormal basis \mathcal{V} , a generic K -sparse function $f \in V$ is uniquely determined by its second moment, up to a global phase.

Proof. The dimension of the representation V is $N = R(L + 1)^2$. Thus, if $R \geq 2L + 1$, then $N = \dim V \geq 2L^3 + 5L^2 + 4L + 1$. On the other hand, since $R \geq \dim V_{\ell}$ for all ℓ , we know by Proposition 3.3 that for $f \in V$ the linear span \mathbb{L}_f of the orbit of f under the ambiguity group $\oplus_{\ell=0}^L O(2\ell + 1)$ has dimension at most

$$\sum_{\ell=0}^L (2\ell + 1)^2 = 4/3L^3 + 4L^2 + 11L/3 + 1.$$

Therefore, by Theorem 3.1, if $K \leq 2/3L^3 + L^2 + L/3$ then for a generic choice of orthonormal basis, a generic K -sparse vector $f \in V$ is uniquely determined by its second moment. \square

Corollary 4.4. Under the conditions of Theorem 4.3, a three-dimensional structure of the form (4.1) can be recovered from n realization from the cryo-EM model when $n = \omega(\sigma^4)$.

Remark 4.5 (Near-optimality). While the sparsity level of Theorem 4.3 is not necessarily optimal, it is optimal up to a constant. Thus, we say that our sparsity bound is near-optimal.

Remark 4.6. A recent paper [24] showed that a three-dimensional structure composed of a finite number of ideal point masses (or its convolution with a fixed kernel with a non-vanishing Fourier transform) can be recovered from the second moment. Theorem 4.3 is far more general as it includes sparse structures under almost any basis. Yet, [24] also suggests an algorithm which harnesses sparsity in the wavelet domain, for which our result does not necessarily hold (since Theorem 4.3 holds for generic bases and we cannot verify that any particular basis satisfies the generic condition).

Remark 4.7 (Spherical-Bessel expansion). Our analysis assumes a model of multiple shells as in (4.1). However, a similar analysis can be carried out to related models, such as spherical-Bessel expansion, where the coefficients $A_\ell^m[r]$ are expanded by

$$A_\ell^m[r] = \sum_{s=1}^{S_\ell} \tilde{A}_\ell^m[s] j_{\ell,s}[r],$$

where the $j_{\ell,s}[r]$ are the normalized spherical Bessel functions. The “bandlimit” S_ℓ is determined by a sampling criterion, akin to Nyquist sampling criterion [27]. This expansion has been useful in various cryo-EM tasks, see for example [58, 16, 25]. Our analysis can be applied to molecular structures represented using the spherical-Bessel expansion, where the only difference is the way we count the dimension of the representation.

5 Crystallographic phase retrieval

The crystallographic phase retrieval problem is the problem of recovering a real signal in \mathbb{R}^N from its power spectrum. As seen from Section 2.4.1, this is equivalent to recovering a real signal from its second moment for the action of either the cyclic group \mathbb{Z}_N or the dihedral group. However, because each irreducible representation appears exactly once, we cannot use Theorem 3.1 to obtain a sparsity bound which ensures generic recovery of signals.

In [19], the authors conjectured that when \mathbb{R}^N is given by the standard basis, a generic K -sparse vector in \mathbb{R}^N can be recovered, up to unavoidable ambiguities, from its power spectrum if $K \leq N/2$. This conjecture was proved for a few specific cases but a complete proof of this conjecture is currently beyond current techniques. In [44], it was shown that for large enough N , a K -sparse, symmetric signals are determined uniquely from their power spectrum for $K = O(N \log^5 N)$.

Here, we rely on previous results on phase retrieval for generic frames and derive the following bound for recovery of vectors contained in a linear subspace.

Theorem 5.1. *Let $K \leq N/2$ and let \mathbb{L} be a generic linear subspace of dimension K . Then, a generic vector $f \in \mathbb{L}$ can be recovered from its power spectrum, up to a global phase.*

Proof. Let \mathbb{L} be a K -dimensional linear subspace of \mathbb{K}^N . Let $f_1, \dots, f_K \in \mathbb{K}^N$ be a basis for \mathbb{L} , and let $h_i = Ff_i \in \mathbb{C}^N$, where F is the $N \times N$ discrete Fourier transform. The vectors $h_1, \dots, h_K \in \mathbb{C}^N$ determine an N -element frame q_1, \dots, q_N on \mathbb{C}^K , where $q_j = (h_{1j}, \dots, h_{Kj})$. If we expand a vector $f \in \mathbb{L}$ as $f = \sum a_i f_i$ with $a_i \in \mathbb{K}$, then the power spectrum of f is exactly the collection of phaseless frame measurements $(|\langle a, q_1 \rangle|^2, \dots, |\langle a, q_N \rangle|^2)$, where $a = (a_1, \dots, a_K) \in \mathbb{K}^K$.

Since the linear subspace \mathbb{L} is arbitrary and the discrete Fourier transform is an isomorphism, for a generic choice of \mathbb{L} the frame q_1, \dots, q_N is generic. By [7, Theorem 3.4], if $N \geq 2K$ the generic vector $a \in \mathbb{K}^K$ can be recovered from these measurements. Therefore, the generic vector $f \in \mathbb{L}$ can be recovered from its power spectrum. \square

Remark 5.2. Note that Theorem 5.1 is weaker than Theorem 3.1, our corresponding results for generic sparsity conditions in the MRA problem, because it is only a statement for a single generic linear subspace as opposed to a generic sparsity condition. In future work, we will pursue an extension of Theorem 5.1 to generic sparsity conditions.

6 Discussion and future work

In this paper, we have derived general sparsity conditions under which the sample complexity of the MRA model (1.1) is only $n = \omega(\sigma^4)$ rather than $n = \omega(\sigma^6)$ in the general case. We have further applied the result to cryo-EM, showing that if a molecular structure can be represented with $\sim N/3$ coefficients in a generic basis, then the sample complexity is quadratic in the variance of the noise.

Next, we delineate a few possible extensions of these results.

Non-compact groups. Our MRA model (1.1) assumes a compact group. However, in some important situations, the group is non-compact, for instance, the group of rigid motions $SE(d)$ [22]. One challenge of working with non-compact groups is that their representations do not necessarily decompose into a sum of irreducibles which makes the representation-theoretic analysis of the second moment more difficult.

Sample complexity for specific bases. Our main theoretical result, Theorem 3.1, holds for almost all bases but it is very difficult to say if they hold for a specific basis, such as wavelets, since the algebraic conditions are implicit. An important future work is to derive conditions for recovery from the second moment for specific bases, and ideally for all bases. (In [25], recovery from the second moment of structures composed of ideal point masses was proven.)

Unified theoretical framework with phase retrieval. In Section 5, Theorem 5.1, we derived sparsity conditions for recovering a signal from its power spectrum, which is the second moment of the simplest MRA model, where a signal in \mathbb{R}^N is acted upon by \mathbb{Z}_N . This problem is called the phase retrieval problem. The proof is based on known results from the phase retrieval literature [7]. We wish to consolidate the proof techniques of Theorem 3.1 and Theorem 5.1 to one general theoretical framework.

Multi-target detection. The multi-target detection model was devised to design a new computational paradigm for recovering small molecular structure using cryo-EM [17]. Without delving into the technical details, the second moment of this model is provided by the diagonals of the matrices B_ℓ , $\ell = 0, \dots, L$, that describe the second moment of the cryo-EM model (4.4) [16]. Deriving the conditions for signal recovery from these diagonals will have important implications to the sample complexity of the multi-target detection model and to understanding the fundamental limitations of the cryo-EM technology.

Alternative priors. This work shows that the sample complexity of MRA and cryo-EM can be significantly improved if the signal can be sparsely represented. An interesting future research thread is studying alternative priors that can improve the sample complexity, such as statistical priors, data-driven priors (e.g., based on AlphaFold [51]), or priors based on the statistical properties of proteins [88, 81].

Acknowledgment

We thank Nicolas Boumal for his notes on [52], and Guy Sharon and Oscar Mickelin for helping, respectively, with Figure 2 and Figure 3. This research is supported by the BSF grant no. 2020159. T.B. is also supported in part by the NSF-BSF grant no. 2019752, and the ISF grant no. 1924/21 and D.E. was also supported by NSF-DMS 1906725 and NSF-DMS 2205626.

References

- [1] Asaf Abas, Tamir Bendory, and Nir Sharon. The generalized method of moments for multi-reference alignment. *IEEE Transactions on Signal Processing*, 70:1377–1388, 2022.
- [2] Emmanuel Abbe, Tamir Bendory, William Leeb, João M Pereira, Nir Sharon, and Amit Singer. Multireference alignment is easier with an aperiodic translation distribution. *IEEE Transactions on Information Theory*, 65(6):3565–3584, 2018.
- [3] Emmanuel Abbe, Joao M Pereira, and Amit Singer. Estimation in the group action channel. In *2018 IEEE International Symposium on Information Theory (ISIT)*, pages 561–565. IEEE, 2018.
- [4] Cecilia Aguerrebere, Mauricio Delbracio, Alberto Bartsaghi, and Guillermo Sapiro. Fundamental limits in multi-image alignment. *IEEE Transactions on Signal Processing*, 64(21):5707–5722, 2016.
- [5] Yariv Aizenbud, Boris Landa, and Yoel Shkolnisky. Rank-one multi-reference factor analysis. *Statistics and Computing*, 31(1):1–31, 2021.
- [6] Kendall Atkinson and Weimin Han. *Spherical harmonics and approximations on the unit sphere: an introduction*, volume 2044. Springer Science & Business Media, 2012.
- [7] Radu Balan, Pete Casazza, and Dan Edidin. On signal reconstruction without phase. *Applied and Computational Harmonic Analysis*, 20(3):345–356, 2006.
- [8] Afonso S Bandeira, Ben Blum-Smith, Joe Kileel, Amelia Perry, Jonathan Weed, and Alexander S Wein. Estimation under group actions: recovering orbits from invariants. *arXiv preprint arXiv:1712.10163*, 2017.
- [9] Afonso S Bandeira, Moses Charikar, Amit Singer, and Andy Zhu. Multireference alignment using semidefinite programming. In *Proceedings of the 5th conference on Innovations in theoretical computer science*, pages 459–470, 2014.
- [10] Afonso S Bandeira, Yutong Chen, Roy R Lederman, and Amit Singer. Non-unique games over compact groups and orientation estimation in cryo-EM. *Inverse Problems*, 36(6):064002, 2020.

- [11] Afonso S Bandeira, Jonathan Niles-Weed, and Philippe Rigollet. Optimal rates of estimation for multi-reference alignment. *Mathematical Statistics and Learning*, 2(1):25–75, 2020.
- [12] Alberto Bartesaghi, Alan Merk, Soojay Banerjee, Doreen Matthies, Xiongwu Wu, Jacqueline LS Milne, and Sriram Subramaniam. 2.2 Å resolution cryo-EM structure of β -galactosidase in complex with a cell-permeant inhibitor. *Science*, 348(6239):1147–1151, 2015.
- [13] Samit Basu and Yoram Bresler. Uniqueness of tomography with unknown view angles. *IEEE Transactions on Image Processing*, 9(6):1094–1106, 2000.
- [14] Tamir Bendory, Alberto Bartesaghi, and Amit Singer. Single-particle cryo-electron microscopy: Mathematical theory, computational challenges, and opportunities. *IEEE signal processing magazine*, 37(2):58–76, 2020.
- [15] Tamir Bendory, Robert Beinert, and Yonina C Eldar. Fourier phase retrieval: Uniqueness and algorithms. In *Compressed Sensing and its Applications*, pages 55–91. Springer, 2017.
- [16] Tamir Bendory, Nicolas Boumal, William Leeb, Eitan Levin, and Amit Singer. Toward single particle reconstruction without particle picking: Breaking the detection limit. *arXiv preprint arXiv:1810.00226*, 2018.
- [17] Tamir Bendory, Nicolas Boumal, William Leeb, Eitan Levin, and Amit Singer. Multi-target detection with application to cryo-electron microscopy. *Inverse Problems*, 35(10):104003, 2019.
- [18] Tamir Bendory, Nicolas Boumal, Chao Ma, Zhizhen Zhao, and Amit Singer. Bispectrum inversion with application to multireference alignment. *IEEE Transactions on Signal Processing*, 66(4):1037–1050, 2017.
- [19] Tamir Bendory and Dan Edidin. Toward a mathematical theory of the crystallographic phase retrieval problem. *SIAM Journal on Mathematics of Data Science*, 2(3):809–839, 2020.
- [20] Tamir Bendory and Dan Edidin. Algebraic theory of phase retrieval. *arXiv preprint arXiv:2203.02774*, 2022.
- [21] Tamir Bendory, Dan Edidin, William Leeb, and Nir Sharon. Dihedral multi-reference alignment. *IEEE Transactions on Information Theory*, 68(5):3489–3499, 2022.
- [22] Tamir Bendory, Ido Hadi, and Nir Sharon. Compactification of the rigid motions group in image processing. *SIAM Journal on Imaging Sciences*, 15(3):1041–1078, 2022.
- [23] Tamir Bendory, Ariel Jaffe, William Leeb, Nir Sharon, and Amit Singer. Super-resolution multi-reference alignment. *Information and Inference: A Journal of the IMA*, 11(2):533–555, 2022.

- [24] Tamir Bendory, Yuehaw Khoo, Joe Kileel, Oscar Mickelin, and Amit Singer. Autocorrelation analysis for cryo-EM with sparsity constraints: Improved sample complexity and projection-based algorithms. *arXiv preprint arXiv:2209.10531*, 2022.
- [25] Tamir Bendory, Oscar Michelin, and Amit Singer. Sparse multi-reference alignment: Sample complexity and computational hardness. In *ICASSP 2022-2022 IEEE International Conference on Acoustics, Speech and Signal Processing (ICASSP)*, pages 8977–8981. IEEE, 2022.
- [26] Tejal Bhamre, Teng Zhang, and Amit Singer. Orthogonal matrix retrieval in cryo-electron microscopy. In *2015 IEEE 12th International Symposium on Biomedical Imaging (ISBI)*, pages 1048–1052. IEEE, 2015.
- [27] Tejal Bhamre, Teng Zhang, and Amit Singer. Anisotropic twicing for single particle reconstruction using autocorrelation analysis. *arXiv preprint arXiv:1704.07969*, 2017.
- [28] Nicolas Boumal. Nonconvex phase synchronization. *SIAM Journal on Optimization*, 26(4):2355–2377, 2016.
- [29] Nicolas Boumal, Tamir Bendory, Roy R Lederman, and Amit Singer. Heterogeneous multireference alignment: A single pass approach. In *2018 52nd Annual Conference on Information Sciences and Systems (CISS)*, pages 1–6. IEEE, 2018.
- [30] Victor-Emmanuel Brunel. Learning rates for Gaussian mixtures under group action. In *Conference on Learning Theory*, pages 471–491. PMLR, 2019.
- [31] Emmanuel J Candès, Justin Romberg, and Terence Tao. Robust uncertainty principles: Exact signal reconstruction from highly incomplete frequency information. *IEEE Transactions on Information Theory*, 52(2):489–509, 2006.
- [32] Hua Chen, Mona Zehni, and Zhizhen Zhao. A spectral method for stable bispectrum inversion with application to multireference alignment. *IEEE Signal Processing Letters*, 25(7):911–915, 2018.
- [33] Yuxin Chen and Emmanuel J Candès. The projected power method: An efficient algorithm for joint alignment from pairwise differences. *Communications on Pure and Applied Mathematics*, 71(8):1648–1714, 2018.
- [34] Ronald R Coifman, Yoel Shkolnisky, Fred J Sigworth, and Amit Singer. Graph Laplacian tomography from unknown random projections. *IEEE Transactions on Image Processing*, 17(10):1891–1899, 2008.
- [35] Jeffrey J Donatelli, Peter H Zwart, and James A Sethian. Iterative phasing for fluctuation X-ray scattering. *Proceedings of the National Academy of Sciences*, 112(33):10286–10291, 2015.
- [36] David L Donoho. Compressed sensing. *IEEE Transactions on Information Theory*, 52(4):1289–1306, 2006.

- [37] Zehao Dou, Zhou Fan, and Harrison Zhou. Rates of estimation for high-dimensional multi-reference alignment. *arXiv preprint arXiv:2205.01847*, 2022.
- [38] Michael Elad. *Sparse and Redundant Representations: From Theory to Applications in Signal and Image Processing*, volume 2. Springer, 2010.
- [39] Yonina C Eldar and Gitta Kutyniok. *Compressed sensing: theory and applications*. Cambridge university press, 2012.
- [40] Carlos Esteve-Yagüe, Willem Diepeveen, Ozan Öktem, and Carola-Bibiane Schönlieb. Spectral decomposition of atomic structures in heterogeneous cryo-EM. *arXiv preprint arXiv:2209.05546*, 2022.
- [41] Zhou Fan, Roy R Lederman, Yi Sun, Tianhao Wang, and Sheng Xu. Maximum likelihood for high-noise group orbit estimation and single-particle cryo-EM. *arXiv preprint arXiv:2107.01305*, 2021.
- [42] Zhou Fan, Yi Sun, Tianhao Wang, and Yihong Wu. Likelihood landscape and maximum likelihood estimation for the discrete orbit recovery model. *Communications on Pure and Applied Mathematics*, 2020.
- [43] Joachim Frank. *Three-dimensional electron microscopy of macromolecular assemblies: visualization of biological molecules in their native state*. Oxford university press, 2006.
- [44] Subhroshekhar Ghosh and Philippe Rigollet. Sparse multi-reference alignment: Phase retrieval, uniform uncertainty principles and the beltway problem. *Foundations of Computational Mathematics*, pages 1–48, 2022.
- [45] Ian Goodfellow, Yoshua Bengio, and Aaron Courville. *Deep learning*. MIT press, 2016.
- [46] Philipp Grohs, Sarah Koppensteiner, and Martin Rathmair. Phase retrieval: uniqueness and stability. *SIAM Review*, 62(2):301–350, 2020.
- [47] Matthew Hirn and Anna Little. Wavelet invariants for statistically robust multi-reference alignment. *Information and Inference: A Journal of the IMA*, 10(4):1287–1351, 2021.
- [48] Shuai Huang, Mona Zehni, Ivan Dokmanić, and Zhizhen Zhao. Orthogonal matrix retrieval with spatial consensus for 3D unknown-view tomography. *arXiv preprint arXiv:2207.02985*, 2022.
- [49] Noam Janco and Tamir Bendory. An accelerated expectation-maximization algorithm for multi-reference alignment. *IEEE Transactions on Signal Processing*, 70:3237–3248, 2022.
- [50] Slavica Jonić and Carlos Óscar Sánchez Sorzano. Coarse-graining of volumes for modeling of structure and dynamics in electron microscopy: Algorithm to automatically control accuracy of approximation. *IEEE Journal of Selected Topics in Signal Processing*, 10(1):161–173, 2015.

- [51] John Jumper, Richard Evans, Alexander Pritzel, Tim Green, Michael Figurnov, Olaf Ronneberger, Kathryn Tunyasuvunakool, Russ Bates, Augustin Žídek, Anna Potapenko, et al. Highly accurate protein structure prediction with AlphaFold. *Nature*, 596(7873):583–589, 2021.
- [52] Zvi Kam. The reconstruction of structure from electron micrographs of randomly oriented particles. *Journal of Theoretical Biology*, 82(1):15–39, 1980.
- [53] Anya Katsevich and Afonso S Bandeira. Likelihood maximization and moment matching in low SNR Gaussian mixture models. *Communications on Pure and Applied Mathematics*, 2020.
- [54] Takeshi Kawabata. Gaussian-input Gaussian mixture model for representing density maps and atomic models. *Journal of structural biology*, 203(1):1–16, 2018.
- [55] Shay Kreymer, Amit Singer, and Tamir Bendory. An approximate expectation-maximization for two-dimensional multi-target detection. *IEEE Signal Processing Letters*, 29:1087–1091, 2022.
- [56] Ti-Yen Lan, Nicolas Boumal, and Amit Singer. Random conical tilt reconstruction without particle picking in cryo-electron microscopy. *Acta Crystallographica Section A*, 78(4):294–301, 2022.
- [57] Chia-Hsueh Lee and Roderick MacKinnon. Structures of the human HCN1 hyperpolarization-activated channel. *Cell*, 168(1-2):111–120, 2017.
- [58] Eitan Levin, Tamir Bendory, Nicolas Boumal, Joe Kileel, and Amit Singer. 3D ab initio modeling in cryo-EM by autocorrelation analysis. In *2018 IEEE 15th International Symposium on Biomedical Imaging (ISBI 2018)*, pages 1569–1573. IEEE, 2018.
- [59] Shuyang Ling. Near-optimal performance bounds for orthogonal and permutation group synchronization via spectral methods. *Applied and Computational Harmonic Analysis*, 60:20–52, 2022.
- [60] Allen Liu and Ankur Moitra. Algorithms from invariants: Smoothed analysis of orbit recovery over $SO(3)$. *arXiv preprint arXiv:2106.02680*, 2021.
- [61] Chao Ma, Tamir Bendory, Nicolas Boumal, Fred Sigworth, and Amit Singer. Heterogeneous multireference alignment for images with application to 2D classification in single particle reconstruction. *IEEE Transactions on Image Processing*, 29:1699–1710, 2019.
- [62] Filipe RNC Maia and Janos Hajdu. The trickle before the torrent—diffraction data from X-ray lasers. *Scientific Data*, 3(1):1–3, 2016.
- [63] Stéphane Mallat. *A wavelet tour of signal processing*. Elsevier, 1999.
- [64] Frank Natterer. *The mathematics of computerized tomography*. SIAM, 2001.

- [65] Thi Hoang Duong Nguyen, Wojciech P Galej, Xiao-chen Bai, Chris Oubridge, Andrew J Newman, Sjors HW Scheres, and Kiyoshi Nagai. Cryo-EM structure of the yeast U4/U6. U5 tri-snRNP at 3.7 Å resolution. *Nature*, 530(7590):298–302, 2016.
- [66] Eva Nogales. The development of cryo-EM into a mainstream structural biology technique. *Nature methods*, 13(1):24–27, 2016.
- [67] Karl Pearson. Contributions to the mathematical theory of evolution. *Philosophical Transactions of the Royal Society of London. A*, 185:71–110, 1894.
- [68] Amelia Perry, Jonathan Weed, Afonso S Bandeira, Philippe Rigollet, and Amit Singer. The sample complexity of multireference alignment. *SIAM Journal on Mathematics of Data Science*, 1(3):497–517, 2019.
- [69] Thomas Pumir, Amit Singer, and Nicolas Boumal. The generalized orthogonal Procrustes problem in the high noise regime. *Information and Inference: A Journal of the IMA*, 10(3):921–954, 2021.
- [70] Ali Punjani, John L Rubinstein, David J Fleet, and Marcus A Brubaker. cryoSPARC: algorithms for rapid unsupervised cryo-EM structure determination. *Nature methods*, 14(3):290–296, 2017.
- [71] Elad Romanov, Tamir Bendory, and Or Ordentlich. Multi-reference alignment in high dimensions: sample complexity and phase transition. *SIAM Journal on Mathematics of Data Science*, 3(2):494–523, 2021.
- [72] David M Rosen, Luca Carlone, Afonso S Bandeira, and John J Leonard. SE-Sync: A certifiably correct algorithm for synchronization over the special Euclidean group. *The International Journal of Robotics Research*, 38(2-3):95–125, 2019.
- [73] DK Saldin, VL Shneerson, Malcolm R Howells, Stefano Marchesini, Henry N Chapman, M Bogan, D Shapiro, RA Kirian, Uwe Weierstall, KE Schmidt, et al. Structure of a single particle from scattering by many particles randomly oriented about an axis: toward structure solution without crystallization? *New Journal of Physics*, 12(3):035014, 2010.
- [74] Sjors HW Scheres. RELION: implementation of a bayesian approach to cryo-EM structure determination. *Journal of structural biology*, 180(3):519–530, 2012.
- [75] Nir Sharon, Joe Kileel, Yuehaw Khoo, Boris Landa, and Amit Singer. Method of moments for 3D single particle ab initio modeling with non-uniform distribution of viewing angles. *Inverse Problems*, 36(4):044003, 2020.
- [76] Yoav Shechtman, Yonina C Eldar, Oren Cohen, Henry Nicholas Chapman, Jianwei Miao, and Mordechai Segev. Phase retrieval with application to optical imaging: a contemporary overview. *IEEE Signal Processing Magazine*, 32(3):87–109, 2015.
- [77] Yoel Shkolnisky and Amit Singer. Viewing direction estimation in cryo-EM using synchronization. *SIAM journal on imaging sciences*, 5(3):1088–1110, 2012.

- [78] Fred J Sigworth. A maximum-likelihood approach to single-particle image refinement. *Journal of structural biology*, 122(3):328–339, 1998.
- [79] Amit Singer. Angular synchronization by eigenvectors and semidefinite programming. *Applied and Computational Harmonic Analysis*, 30(1):20–36, 2011.
- [80] Amit Singer. Mathematics for cryo-electron microscopy. In *Proceedings of the International Congress of Mathematicians: Rio de Janeiro 2018*, pages 3995–4014. World Scientific, 2018.
- [81] Amit Singer. Wilson statistics: derivation, generalization and applications to electron cryomicroscopy. *Acta Crystallographica Section A: Foundations and Advances*, 77(5), 2021.
- [82] Amit Singer and Yoel Shkolnisky. Three-dimensional structure determination from common lines in cryo-EM by eigenvectors and semidefinite programming. *SIAM journal on imaging sciences*, 4(2):543–572, 2011.
- [83] Amit Singer and Fred J Sigworth. Computational methods for single-particle electron cryomicroscopy. *Annual Review of Biomedical Data Science*, 3:163, 2020.
- [84] Amit Singer and H-T Wu. Two-dimensional tomography from noisy projections taken at unknown random directions. *SIAM journal on imaging sciences*, 6(1):136–175, 2013.
- [85] John CH Spence, Uwe Weierstall, and HN Chapman. X-ray lasers for structural and dynamic biology. *Reports on Progress in Physics*, 75(10):102601, 2012.
- [86] Robert Tibshirani. Regression shrinkage and selection via the lasso. *Journal of the Royal Statistical Society: Series B (Methodological)*, 58(1):267–288, 1996.
- [87] Cédric Vonesch, Lanhui Wang, Yoel Shkolnisky, and Amit Singer. Fast wavelet-based single-particle reconstruction in cryo-EM. In *2011 IEEE International Symposium on Biomedical Imaging: From Nano to Macro*, pages 1950–1953. IEEE, 2011.
- [88] AJC Wilson. The probability distribution of X-ray intensities. *Acta Crystallographica*, 2(5):318–321, 1949.
- [89] Wilson Wong, Xiao-chen Bai, Alan Brown, Israel S Fernandez, Eric Hanssen, Melanie Condrón, Yan Hong Tan, Jake Baum, and Sjors HW Scheres. Cryo-EM structure of the Plasmodium falciparum 80S ribosome bound to the anti-protozoan drug emetine. *Elife*, 3:e03080, 2014.
- [90] Mona Zehni, Shuai Huang, Ivan Dokmanić, and Zhizhen Zhao. 3D unknown view tomography via rotation invariants. In *ICASSP 2020-2020 IEEE International Conference on Acoustics, Speech and Signal Processing (ICASSP)*, pages 1449–1453. IEEE, 2020.
- [91] Mona Zehni and Zhizhen Zhao. An adversarial learning based approach for 2D unknown view tomography. *IEEE Transactions on Computational Imaging*, 8:705–720, 2022.

A Representation theory

A.1 Terminology on representations

Let G be a group. A (complex) representation of G is a homomorphism, $G \xrightarrow{\pi} \text{GL}(V)$, where V is a complex vector space and $\text{GL}(V)$ is the group of invertible linear transformations $V \rightarrow V$. Given a representation of a group G , we can define an action of G on V by $g \cdot v = \pi(g)v$. Since $\pi(g)$ is a linear transformation, the action of G is necessarily linear, meaning that for any vectors v_1, v_2 and scalars $\lambda, \mu \in \mathbb{C}$ $g \cdot (\lambda v_1 + \mu v_2) = \lambda(g \cdot v_1) + \mu(g \cdot v_2)$. Conversely, given a linear action of G on a vector space V , we obtain a homomorphism $G \rightarrow \text{GL}(V)$, $g \mapsto T_g$, where $T_g: V \rightarrow V$ is the linear transformation $T_g(v) = (g \cdot v)$. Thus, giving a representation of G is equivalent to giving a linear action of G on a vector space V . Given this equivalence, we will follow standard terminology and refer to a vector space V with a linear action of G as a *representation of G* .

A representation V of G is *finite dimensional* if $\dim V < \infty$. In this case, a choice of basis for V identifies $\text{GL}(V) = \text{GL}(N)$, where $N = \dim V$. Given a Hermitian inner product $\langle \cdot, \cdot \rangle$ on V , we say that a representation is *unitary* if for any two vectors $v_1, v_2 \in V$ $\langle g \cdot v_1, g \cdot v_2 \rangle = \langle v_1, v_2 \rangle$. If we choose an orthonormal basis for V , then the representation of G is unitary if and only if the image of G under the homomorphism $G \rightarrow \text{GL}(N)$ lies in the subgroup $U(N)$ of unitary matrices.

A representation V of a group G is *irreducible* if V contains no non-zero proper G -invariant subspaces.

A.2 Representations of compact groups

Any compact group G has a G -invariant measure called a Haar measure. The Haar measure dg is typically normalized so that $\int_G dg = 1$. If V is a finite-dimensional representation of a compact group and (\cdot, \cdot) is any Hermitian inner product, then the inner product $\langle \cdot, \cdot \rangle$ defined by the formula $\langle v_1, v_2 \rangle = \int_G (g \cdot v_1, g \cdot v_2) dg$ is G -invariant. As a consequence we obtain the following fact.

Proposition A.1. *Every finite dimensional representation of a compact group is unitary.*

Using the invariant inner product we can then obtain the following decomposition theorem for finite dimensional representations of compact group.

Proposition A.2. *Any finite dimensional representation of a compact group decomposes into a direct sum of irreducible representations.*

If V is a representation, then $V^G = \{v \in V | g \cdot v = v\}$ is a subspace which is called the subspace of invariants.

A.3 Schur's Lemma

A key property of irreducible unitary representations is Schur's Lemma. Recall that a linear transformation Φ is G -invariant if $g \cdot \Phi v = \Phi g \cdot v$.

Lemma A.3. *Let $\Phi: V_1 \rightarrow V_2$ be a G -invariant linear transformation of finite dimensional irreducible representations of a group G (not necessarily compact). Then, Φ is either zero or an isomorphism. Moreover, if V is a finite dimensional irreducible unitary representation of a group G then any G -invariant linear transformation $\phi: V \rightarrow V$ is multiplication by a scalar.*

A.4 Dual, Hom and tensor products of representations

If V_1 and V_2 are representations of a group G , then the vector space $\text{Hom}(V_1, V_2)$ of linear transformations $V_1 \rightarrow V_2$ has a natural linear action of G given by the formula $(g \cdot A)(v_1) = g \cdot A(g^{-1}v_1)$. In particular, if V is a representation of G , then $V^* = \text{Hom}(V, \mathbb{C})$ has a natural action of G given by the formula $(g \cdot f)(v) = f(g^{-1}v)$.

A choice of inner product on V determines an identification of vector spaces $V = V^*$, given by the formula $v \mapsto \langle \cdot, v \rangle$. If V is a unitary representation of G then with the identification of $V = V^*$ the dual action of G on V is given by the formula $g \cdot_* v = \bar{g} \cdot v$. Likewise, if V_1 and V_2 are two representations then we can define an action of G on $V_1 \otimes V_2$ by the formula $g \cdot (v_1 \otimes v_2) = (g \cdot v_1) \otimes (g \cdot v_2)$.

Given two representations spaces V_1, V_2 there is an isomorphism of representations $V_1 \otimes V_2^* \rightarrow \text{Hom}(V_2, V_1)$ given by the formula $v_1 \otimes f_2 \mapsto \phi$, where the linear transform $\phi: V_2 \rightarrow V_1$ is defined by the formula $\phi(v_2) = f_2(v_2)v_1$. In particular, we can identify $V \otimes V^*$ with $\text{Hom}(V, V)$.